c-Axis Dimer and Its Electronic Breakup: The Insulator-to-Metal Transition in Ti$_2$O$_3$

C. F. Chang,[1] T. C. Koethe,[2] Z. Hu,[1] J. Weinen,[1] S. Agrestini,[1] L. Zhao,[1] J. Gegner,[2] H. Ott,[2] G. Panaccione,[3]
Hua Wu,[4] M. W. Haverkort,[5] H. Roth,[2] A. C. Komarek,[1] F. Offi,[6] G. Monaco,[7,*] Y.-F. Liao,[8]
K.-D. Tsuei,[8] H.-J. Lin,[8] C. T. Chen,[8] A. Tanaka,[9] and L. H. Tjeng[1]

[1]*Max Planck Institute for Chemical Physics of Solids, Nöthnitzer Straße 40, 01187 Dresden, Germany*
[2]*Institute of Physics II, University of Cologne, Zülpicher Straße 77, 50937 Cologne, Germany*
[3]*TASC Laboratory, IOM-CNR, Area Science Park, S.S.14, Km 163.5, I-34149 Trieste, Italy*
[4]*Laboratory for Computational Physical Sciences (MOE), State Key Laboratory of Surface Physics,
and Department of Physics, Fudan University, Shanghai 200433, People's Republic of China*
[5]*Institute for Theoretical Physics, Heidelberg University, Philosophenweg 19,
69120 Heidelberg, Germany*
[6]*CNISM and Dipartimento di Scienze, Università Roma Tre,
Via della Vasca Navale 84, I-00146 Rome, Italy*
[7]*European Synchrotron Radiation Facility, BP220, 38043 Grenoble, France*
[8]*National Synchrotron Radiation Research Center, 101 Hsin-Ann Road, Hsinchu 30076, Taiwan*
[9]*Department of Quantum Matter, ADSM, Hiroshima University, Higashi-Hiroshima 739-8530, Japan*

We report on our investigation of the electronic structure of Ti$_2$O$_3$ using (hard) x-ray photoelectron and soft x-ray absorption spectroscopy. From the distinct satellite structures in the spectra, we have been able to establish unambiguously that the Ti-Ti c-axis dimer in the corundum crystal structure is electronically present and forms an $a_{1g}a_{1g}$ molecular singlet in the low-temperature insulating phase. Upon heating, we observe a considerable spectral weight transfer to lower energies with orbital reconstruction. The insulator-metal transition may be viewed as a transition from a solid of isolated Ti-Ti molecules into a solid of electronically partially broken dimers, where the Ti ions acquire additional hopping in the a-b plane via the e_g^π channel, the opening of which requires consideration of the multiplet structure of the on-site Coulomb interaction.

Subject Areas: Condensed Matter Physics,
Strongly Correlated Materials

The role of ion pair formation for the metal-insulator transition (MIT) in early transition metal oxides, with the octahedra sharing either a common face or a common edge, has been a matter of debate in the past several decades [1–21]. Based on the presence of the c-axis V–V dimers in the corundum crystal structure of V$_2$O$_3$, Castellani *et al.* [4] proposed a molecular singlet model for the a_{1g} orbitals, projecting the system effectively onto a solid with $S = 1/2$ entities, which then should carry the essential physics for the MIT and the magnetic structure in the antiferromagnetic insulating phase. However, soft x-ray absorption spectroscopy (XAS) experiments [10] showed that the two d

electrons on each V are in the high-spin $S = 1$ state, implying that the atomic Hund's rule coupling is much stronger than the intradimer hopping integrals. Furthermore, using band structure calculations, Elfimov *et al.* [12] found that the intradimer hopping integral is not the most important one; rather, the hopping integrals between second, third, and fourth nearest V neighbors are at least equally important. In other words, the c-axis dimers need not be present electronically, although structurally they are present.

Ti$_2$O$_3$ shares much of the same fascination as V$_2$O$_3$. It also has a corundum crystal structure (see the inset in Fig. 1) and exhibits, upon lowering the temperature, a MIT [22]. The earliest models explained the low-temperature insulating phase of Ti$_2$O$_3$ by assuming a band splitting caused by an antiferromagnetic long-range order [22]. However, in contrast to V$_2$O$_3$, the transition is gradual and is not accompanied by a structural transition nor magnetic ordering [23–25]. Goodenough and Van Zandt *et al.* also proposed that the short c-axis pair bond length of 2.578 Å at 300 K [26], which is much shorter than in V$_2$O$_3$, with 2.697 Å at 300 K [27], increases the trigonal crystal
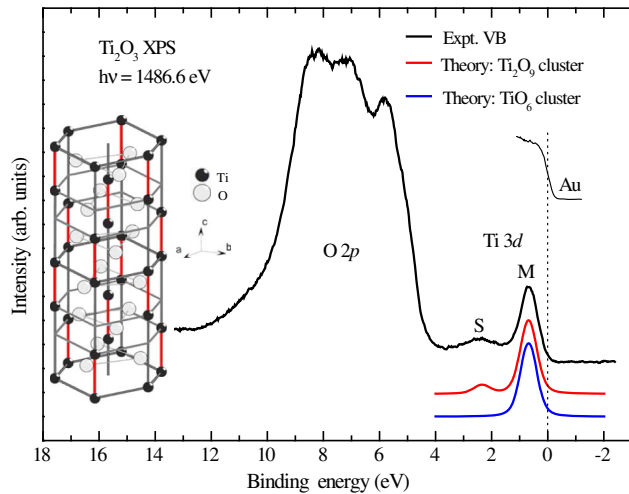
FIG. 1. Experimental valence-band (VB) XPS spectrum of Ti_2O_3 taken at 300 K (black line), together with the Au Fermi cutoff (thin black line) as reference for E_F. Also shown is the Ti $3d$ one-electron removal spectrum from the TiO_6 (blue line) and the Ti_2O_9 (red line) clusters, as described in the text. Inset: Corundum structure of Ti_2O_3, with the c-axis Ti-Ti dimers marked in red.

field splitting so that the conductivity gap is opened [1,2]. However, this model is contradicted by band structure calculations, which showed that the overlap of the a_{1g} and e_g^π orbitals can only be suppressed for an unrealistically short bond length [8]; i.e., Ti_2O_3 is a metal at all temperatures, with mixed a_{1g}-e_g^π states for the c-axis dimer from the point of view of band theory [8,15]. Correlation effects have to be included in one way or another to explain the insulating ground state in Ti_2O_3 [3,13,14,28–30].

Here, we report on our spectroscopic study of the electronic structure of Ti_2O_3, with the goal to determine whether and how correlation effects and the c-axis dimer play a role for the formation of the low-temperature insulating phase. Moreover, we would like to identify the key factors in the electronic structure that can transform the compound from an insulator into a metal. In our spectra, we find direct evidence that Ti_2O_3 is a strongly correlated system in which the c-axis Ti-Ti dimers form isolated $a_{1g}a_{1g}$ molecular singlets at low temperatures, and that at high temperatures the dimers partially break up electronically, with the Ti ions gaining hopping in the a-b plane via the e_g^π channel. It is crucial that the orbital switching from a_{1g} towards e_g^π is possible only if the multiplet aspect of the on-site Coulomb interaction is another decisive element in the electronic structure of Ti_2O_3.

X-ray photoelectron spectroscopy (XPS) measurements with $h\nu = 1486.6$ eV were performed in Cologne using a Vacuum Generators twin-crystal monochromatized Al-$K\alpha$ source and a Scienta SES-100 electron energy analyzer. The overall energy resolution was set to 0.4 eV. Hard x-ray photoelectron spectroscopy (HAXPES) experiments were

carried out at the ID16 beam line of the European Synchrotron Radiation Facility (ESRF) using the VOLume PhotoEmission from solids (VOLPE) spectrometer with $h\nu = 5931$ eV and an overall resolution of 0.4 eV, as well as at the Taiwan beam line BL12XU at SPring-8 using the Max-Planck-National Synchrotron Radiation Research Center (NSRRC) end station equipped with a MB Scientific A-1 HE hemispherical analyzer employing $h\nu \simeq 6.5$ keV and an overall resolution of 0.2 eV. Soft-x-ray absorption spectra (XAS) were collected at the Dragon beam line at the NSRRC in Taiwan in the total electron yield mode, with a photon energy resolution of 0.25 eV and a degree of linear polarization of 98%. All spectra were collected from freshly *in vacuo* cleaved Ti_2O_3 single crystals. Ti_2O_3 single crystals were grown by using the floating zone method. The purity and structure of crystals were verified as a single phase crystal by using energy-dispersive x-ray spectroscopy (EDX), powder diffraction measurements, Laue, and polarization microscopy. The stoichiometry of the crystals has been characterized by thermogravimetric analysis. The temperature-dependent resistivity from 10 K to 575 K of the Ti_2O_3 crystals shows the insulator-to-metal transition (see Fig. 5 of Appendix A).

Figure 1 displays the valence-band XPS spectrum of Ti_2O_3 taken at 300 K, i.e., in the insulating phase. The group of peaks at 4–11-eV binding energies is mainly the contribution of O $2p$ states. The lower-binding-energy region from the Fermi level up to 4 eV consists of mainly the Ti $3d$. This part of the spectrum is characterized by two distinct spectral features. The main line (M) is a quite symmetric peak centered at about 0.68 eV with a width of approximately 0.8 eV (FWHM). The semiconducting or insulating nature of Ti_2O_3 at room temperature [2,31,32] is reflected by the fact that the spectral weight vanishes at the Fermi level, in agreement with earlier photoemission reports [33–38] and the observation of a 0.2-eV gap in the optical conductivity [20,39].

The second feature is a somewhat broader but clearly noticeable satellite (S) at around 2.43-eV binding energy. The origin of this peak has so far been disputed. Ultraviolet photoelectron spectroscopy (UPS) studies speculated that it was a surface state with a considerable $3d$ band character [33,34]. However, an angle-resolved UPS study was not able to confirm this speculation [35]. We claim here that our spectrum is representative of the bulk material, i.e., that both features M and S belong to the photoemission spectrum of bulk Ti_2O_3. This relies on the fact that our spectrum was taken on a cleaved single crystal at normal emission, with a photon energy of 1486.6 eV, thereby obtaining larger probing depths [40–42]. Below, in the paragraphs concerning the Ti $2p$ core-level, we also provide more spectroscopic evidence that all our spectra are representative for the bulk.

The absence of any spectral weight at the Fermi level in the low-temperature phase of Ti_2O_3 invalidates the

predictions of band structure calculations [8,15], which always display a finite density of states at the Fermi level. This is a strong sign that correlation effects play a crucial role. However, the hybrid functional and nonlocal exchange calculations [28–30] failed to produce a satellite structure like the feature S that we have observed at 2.43-eV binding energy. A two-site cluster dynamical mean-field theory (DMFT) calculation, on the other hand [14], did produce a satellite structure but with an intensity that was much too low. Here, we infer that a quantitative explanation for the satellite structure is a necessity to construct a realistic model for the MIT in Ti_2O_3.

In order to unveil the origin of the satellite structure S, we now resort to configuration-interaction cluster calculations with full atomic multiplet theory, an approach that is very successful to quantitatively explain the basic features in many photoelectron and x-ray absorption spectra of $3d$ transition metal oxides [43–46]. We start with the standard single transition-metal-site cluster, i.e., a TiO_6 octahedral cluster with the Ti ion in the center [38], and we use model parameters that are typical for titanium oxides [14,44,47,48]. We find that the Ti $3d$ one-electron removal spectrum near the Fermi level consists of a single peak (see the blue curve in Fig. 1). Satellite S is not reproduced in a single-site cluster. Next, motivated by the presence of the Ti-Ti c-axis dimer in the crystal structure, we calculate the spectrum of a Ti_2O_9 cluster consisting of two face-shared TiO_6 octahedral units along the c axis, using the same parameters as for the TiO_6 cluster but with the addition of a parameter describing the inter-Ti hopping [48]. The result is given by the red curve in Fig. 1, and we can observe that both the satellite structure S and the main peak M can be reproduced very well.

To interpret this result, we can use the following schematic model. The relevant orbital in this Ti-Ti dimer is the one pointing along the bond, namely, a_{1g}. With each Ti ion having the 3+ valence, we then consider the following singlet configurations forming the ground state: $a_{1gA}a_{1gB}$, $a_{1gA}a_{1gA}$, and $a_{1gB}a_{1gB}$, where A and B denote the two Ti sites. The configurations with the double occupation on one site have the extra energy Hubbard U, and the hopping integral between the a_{1gA} and a_{1gB} orbitals is denoted by t. This is basically the Hubbard model for a hydrogen molecule as described by Ashcroft and Mermin [49], with further details given in Appendix B. The photoemission final states, in which one electron has been removed, are given by the following two configurations, namely, a_{1gA} and a_{1gB}, which are degenerate in energy and form bonding and antibonding states with energies $-t$ and $+t$. See Fig. 6 of Appendix B. Their energy separation $2t$ can then be read directly from the energy separation between feature M and S, i.e., $2t = 1.75$ eV ($t = 0.88$ eV). The intensity ratio between M and S is determined by U/t. See Appendix B. For $U/t = 0$, the
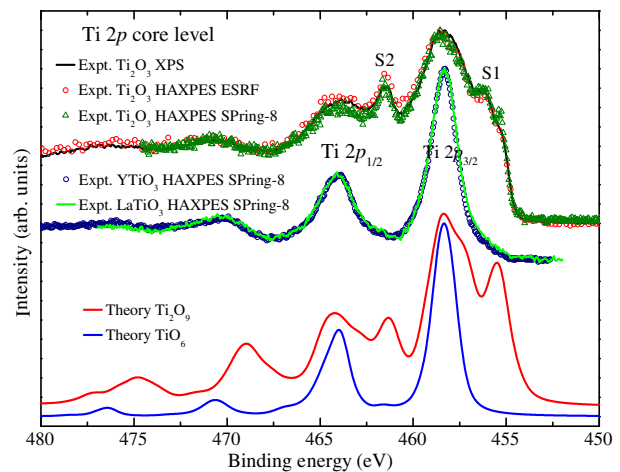

FIG. 2. Experimental Ti $2p$ core-level photoemission spectra of Ti_2O_3 taken at 300 K with $h\nu = 1486.6$ eV (black line, XPS), $h\nu = 5931$ eV (red circle, HAXPES ESRF), and $h\nu \simeq 6500$ eV (dark-green triangle symbol, HAXPES SPring-8), and experimental Ti $2p$ core-level photoemission spectra of $YTiO_3$ taken at 300 K (navy circle) and of $LaTiO_3$ taken at 200 K (green line) with $h\nu \simeq 6500$ eV (HAXPES SPring-8). Also shown are the theoretical configuration-interaction calculations using the TiO_6 (blue line) and the Ti_2O_9 (red line) clusters; see text.

intensity of the satellite S vanishes, and we return to the one-electron approximation. In the limit of $U/t \to \infty$, M and S will have equal intensities. From the experimental intensity ratios, we estimate that U/t is about 3–4, i.e., $U \approx 2.5$–3.5 eV. Thus, the essential outcome of the Ti_2O_9 cluster calculation is that the intersite Ti hopping, together with the on-site Coulomb interaction, produces a main line M with a satellite structure S, and that the presence of M and S shows that there is a strong electronic bond between the two Ti ions of the dimer.

In order to collect more evidence for the presence of the strong electronic bond within the Ti-Ti c-axis dimer, we now investigate the Ti $2p$ core-level spectrum. Figure 2 shows the Ti $2p$ core-level spectrum of Ti_2O_3 taken at 300 K with $h\nu = 1486.6$ eV (black line, XPS), $h\nu = 5931$ eV (red circle, HAXPES ESRF), and $h\nu \simeq 6500$ eV (dark-green triangle symbol, HAXPES SPring-8), together with the Ti $2p$ spectra from $YTiO_3$ (navy circle) and $LaTiO_3$ (green line) with $h\nu \simeq 6500$ eV (HAXPES SPring-8). The first aspect we mention is that the Ti_2O_3 XPS spectrum is identical to the bulk-sensitive Ti_2O_3 HAXPES spectra taken at ESRF and SPring-8. This demonstrates that our XPS spectra, i.e., also the ones displayed in Fig. 1, are representative of the bulk material. The Ti $2p$ core-level XPS spectra reported so far in the literature [38,50] have a line shape that is different from ours. We have therefore carried out the Ti $2p$ experiment multiple times, using different batches of Ti_2O_3 samples and using the XPS in our home laboratory as well as the more bulk-sensitive HAXPES at two different experimental
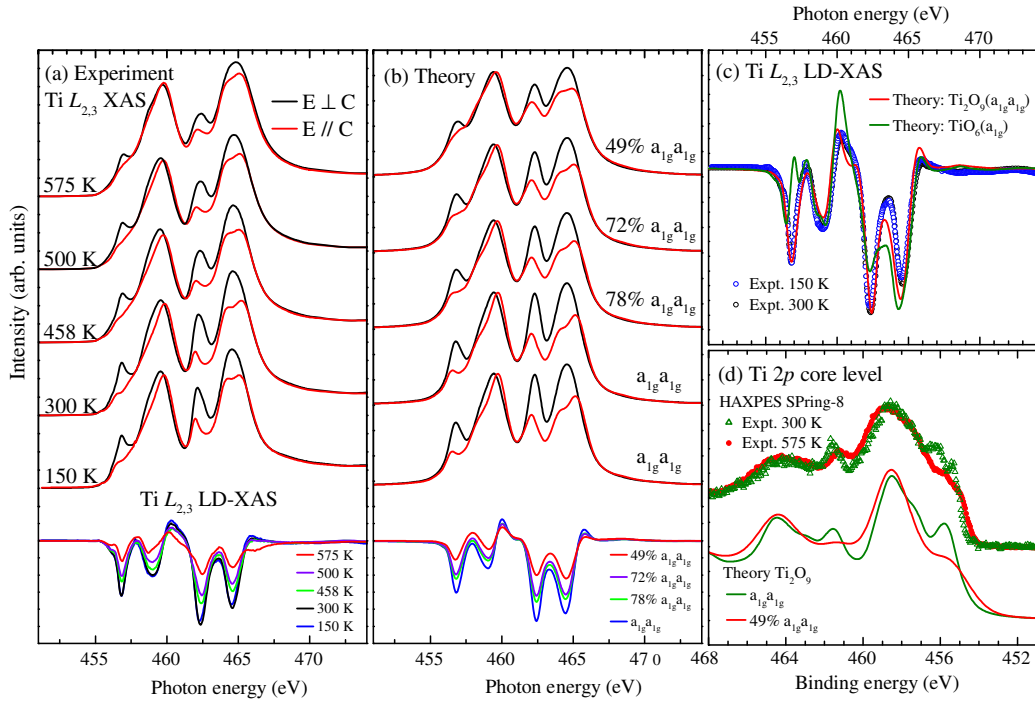
FIG. 3.   Panel (a): Experimental polarization-dependent Ti-$L_{2,3}$ XAS spectra of Ti_2O_3 taken at 150 K, 300 K, 458 K, 500 K, and 575 K. Panel (b): Calculated polarization-dependent Ti-$L_{2,3}$ XAS spectra for the corresponding temperatures using the Ti_2O_9 cluster. In the bottom of panels (a) and (b) are the corresponding linear dichroic (LD) spectra. Panel (c): Close-up of the experimental LD spectrum in the low-temperature phase (blue and black circles) and the simulation using the TiO_6 (green line: a_{1g}) and the Ti_2O_9 (red line: $a_{1g}a_{1g}$) clusters. Panel (d): Temperature dependence of the Ti $2p$ core-level spectrum and the simulations using the Ti_2O_9 cluster.

stations (ESRF and SPring8), all to verify that the spectra we were collecting are indeed reproducible. The second aspect to notice is that the Ti_2O_3 spectra are very different from those of $YTiO_3$ and $LaTiO_3$, despite the fact that all are Ti^{3+} $3d^1$ compounds. The satellites marked as $S1$ and $S2$ have truly massive intensities, indicative of essential differences in the local electronic structure between Ti_2O_3 and $YTiO_3/LaTiO_3$.

To quantify the observations, we calculate the Ti $2p$ electron removal spectrum using the single-site Ti cluster, i.e., TiO_6, and the two-site Ti cluster, i.e., Ti_2O_9, as described above. The result for the TiO_6 cluster is shown by the blue line in Fig. 2: The calculated spectrum is essentially similar to the one reported in Ref. [38], and it reproduces the $YTiO_3$ and $LaTiO_3$ spectra excellently. The result for the Ti_2O_9 cluster is quite different from that of the TiO_6 cluster, and it matches very well the experimental Ti_2O_3 spectra, including the high-intensity satellite features $S1$ and $S2$. These findings show that the Ti ions in $YTiO_3$ and $LaTiO_3$ are relatively isolated, while in Ti_2O_3, they form electronically very strongly bonded pairs, fully consistent with the analysis for the valence-band spectrum discussed above.

Having established the electronic presence of the c-axis dimers, we need to determine or verify that the relevant

orbitals that form the bond are the Ti a_{1g}. We also need to investigate how this orbital occupation may evolve as a function of temperature across the insulator-metal transition. Figure 3(a) shows the polarization-dependent Ti $L_{2,3}$ XAS spectra of Ti_2O_3 taken at 150 K, 300 K, 458 K, 500 K, and 575 K, i.e., from deep in the insulating low-temperature phase, across the gradual insulator-metal transition, and well into the metallic high-temperature phase. We can observe a strong polarization dependence indicative of a distinct orbital occupation of the Ti $3d$ shell. We also notice that the polarization dependence decreases across the transition. In order to quantitatively extract the orbital occupation of the Ti $3d$ states from these Ti $L_{2,3}$ XAS spectra, we simulated the spectra using the Ti_2O_9 cluster. The results are shown in Fig. 3(b) We can clearly observe the excellent overall match between experiment and theory for all temperatures.

Focusing first on the low-temperature phase, we find that the 150-K and 300-K spectra can be very well described by a Ti-Ti c-axis dimer in an essentially pure $a_{1g}a_{1g}$ singlet ground state. In addition, a close-up look at the dichroic spectrum—i.e., the difference between the spectrum taken with $\mathbf{E} \parallel c$ and the spectrum with $\mathbf{E} \perp c$ spectra, where $\mathbf{E}$ denotes the electric field vector of the incoming light—shows that the $a_{1g}a_{1g}$ ground state

reproduces the experiment in great detail; see Fig. 3(c) (experiment, blue and black dots; simulation, red line). By contrast, a single-site TiO_6 cluster with an a_{1g} initial state produces a significantly poorer fit (green line). The low-temperature XAS spectra thus not only fully confirm the findings from the photoemission experiments shown above about the strong intradimer electronic bond but also show that this bond is formed by the $a_{1g}a_{1g}$ singlet.

With this finding, we in fact restore the presumptions of the early model by Goodenough and Van Zandt *et al.* [1,2] for the insulating state, namely, that the ground state is given by the dimer in the $a_{1g}a_{1g}$ singlet. This model has been rejected for decades by band structure calculations [8,15] on the basis that these calculations found a heavily mixed orbital occupation. We also completely validate the starting point of the Mott-Hubbard model by Tanaka [13], thereby correcting the numbers found in an earlier polarization-dependent Ti $L_{2,3}$ XAS experiment [19]: By extending our experiment to lower temperatures, we ensure that our low-temperature spectrum is taken from deep inside the insulating phase, and by including the O $2p$ ligands in our analysis, we are able to obtain a better match between the simulation and experiment, as shown in Fig. 3(c).

Concerning the temperature evolution, the decrease in the size of the linear dichroism [see the bottom panel of Fig. 3(a)] across the gradual insulator-metal transition can be ascribed to a reconstruction of the Ti $3d$ orbital occupation [2,3,13,19]. Our simulations, both the polarization-dependent and dichroic spectra, find that the occupation of the $a_{1g}a_{1g}$ singlet state is reduced to 78%, 72%, and 49% for $T = 458$ K, 500 K, and 575 K, respectively. The e_g^{π} orbitals of the Ti t_{2g} shell become more and more occupied. The Ti ion thus becomes electronically less anisotropic, thereby also weakening and eventually breaking the electronic bond of the *c*-axis dimer. This is mirrored by the strong changes in the Ti $2p$ core-level spectrum and, in particular, in the reduction of the intensities of the satellites S1 and S2, which are well captured by the same model used for calculating the temperature-dependent XAS spectra [see Fig. 3(d)]. In addition, the lengthening of the *c*-axis dimer bond distance [51] across the gradual insulator-metal transition can be viewed as a weakening of the bond.

The partial breakup of the dimer and the orbital reconstruction with temperature have consequences for the states closest to the chemical potential. In the left panel of Fig. 4, we display a close-up of the valence band collected with the bulk-sensitive HAXPES method, and in the right panel, we show the threshold region of the O K-edge XAS as an indicator for the unoccupied states. We clearly observe the gradual closing of the band gap. Perhaps more striking is the fact that spectral weight is transferred over an energy range of 0.3 eV on both sides of the chemical potential. Similar effects can also be seen in
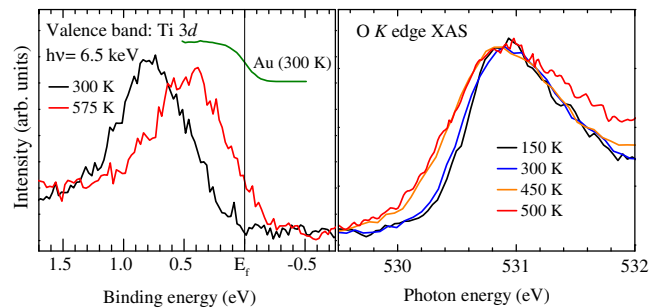

FIG. 4.   Left panel: Close-up of the temperature dependence of the valence-band spectra of Ti_2O_3 taken with $h\nu \simeq 6.5$ keV (HAXPES SPring-8), together with the Au Fermi cutoff as E_F reference. Right panel: Close-up of the temperature dependence of the O K-edge XAS spectra of Ti_2O_3.

the optical conductivity [20]. One may try to explain these changes in terms of large shifts in the energies of the relevant orbitals [2,3,20] or perhaps also in terms of large changes in the strength of the intradimer hopping integrals, but the density of states from band structure calculations [8,28,30] shows only modest changes with temperature. The large discrepancy between the energy scale of the transition temperature (ca. 0.04 eV) and the energy scale over which spectral weight is transferred (0.3–0.4 eV) indicates clearly that mean-field theories cannot be applied to explain the MIT.

Therefore, we have to take strong electron correlation effects explicitly into account in the explanation, so small changes in the one-electron bandwidth and in the strength of the effective Coulomb interaction U_{eff} can lead to large changes in the electronic structure, e.g., a MIT with a large transfer of spectral weight. The key issue for Ti_2O_3 is the orbital reconstruction away from a pure $a_{1g}a_{1g}$ dimer singlet state at low temperatures. Those dimers are electronically isolated from each other in the solid: The hopping in the *a-b* plane for electrons in the a_{1g} orbital (oriented along the *c* axis) is small (≤ 1 eV [15,30]) compared to the Coulomb energy $U_{\text{eff}} = U$, where U (≈ 3 eV, see above) is the energy repulsion between two electrons doubly occupying the same a_{1g} orbital of one particular Ti site after such a hopping process occurs in the plane.

If, on the other hand, the electrons are also allowed to occupy the e_g^{π} orbitals, then the hopping in the *a-b* plane will be greatly enhanced, simply because the e_g^{π} orbitals are much more directed in this plane. Moreover, after such a hopping, the doubly occupied state can be a triplet (high-spin) $a_{1g}e_g^{\pi}$. The effective Coulomb energy U_{eff} will then be given by U'-J_H, where J_H denotes the gain in Hund's rule exchange energy for pairs of spin-parallel electrons and where U' is the energy repulsion between electrons in different orbitals, to be distinguished from U, which is that for electrons in the same orbital. Note that U' is smaller than U by about $2J_H$, so for the $a_{1g}e_g^{\pi}$ situation, U_{eff} is smaller by

an amount $3J_H$ than the U_{eff} for $a_{1g}a_{1g}$. Considering that J_H is typically 0.7 eV [44], U_{eff} for $a_{1g}e_g^\pi$ can be 2.1 eV smaller than that for $a_{1g}a_{1g}$. So, for the $a_{1g}e_g^\pi$ situation, the e_g^π bandwidth in the a-b plane (≈ 1.5 eV [15,30]) can overcome U_{eff} (≈ 0.9 eV) to stabilize a metallic state.

To justify that converting a dimer in the singlet $a_{1g}a_{1g}$ situation into a dimer with the triplet $a_{1g}e_g^\pi$ requires only a modest amount of energy, we need to estimate the dimer's total energy in each situation. Hereby, we follow a perturbative approach analogous to the one often used to estimate superexchange interactions in transition metal oxides. For $a_{1g}a_{1g}$, the hopping between the state with one electron on each Ti and the state with one of the Ti doubly occupied and the other empty is given by $(\sqrt{2})^2 t_{a1g}$ (there are two ways to obtain the first state from each of the latter states, giving each the $\sqrt{2}$ factor). Here, U_{eff} is given by U (see above). For $a_{1g}e_g^\pi$, the hopping between the state with one electron on each Ti and the state with one of the Ti doubly occupied and the other empty is given by t_{a1g} (here, we neglect the hopping of the e_g^π along the c axis completely). The U_{eff} is $U' - J_H$ (see above). Thus, whereas for $a_{1g}a_{1g}$ both the hopping and U_{eff} are large, for $a_{1g}e_g^\pi$ both the hopping and U_{eff} are small. One can therefore argue that, together with lattice effects, one can find physically reasonable parameters to keep the total energy difference between the two situations within 0.1 eV. These findings provide strong experimental support for the theoretical model proposed by Tanaka [13] to explain the MIT in Ti_2O_3.

To summarize, using a combination of photoelectron and polarized x-ray absorption spectroscopy, we were able to establish that the low-temperature phase of Ti_2O_3 can be viewed as a collection of isolated c-axis Ti-Ti dimers in the singlet $a_{1g}a_{1g}$ configuration. Upon heating and crossing the gradual insulator-metal transition, the dimers start to break up with a reconstruction of the orbital occupation. The availability of the e_g^π channel increases the hopping within the a-b plane. The smaller effective Coulomb interaction for the triplet $a_{1g}e_g^\pi$ configuration facilitates the orbital reconstruction and the stabilization of the metallic state at high temperatures.

ACKNOWLEDGMENTS

APPENDIX A: RESISTIVITY (T)

Figure 5 shows the temperature-dependent resistivity of Ti_2O_3 from 10 K to 575 K. The insulator-to-metal transition can be seen.
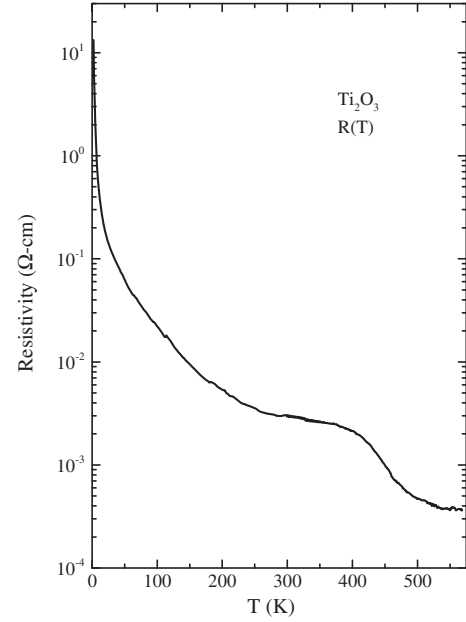

FIG. 5. Temperature-dependent resistivity of Ti_2O_3 from 10 K to 575 K, showing the insulator-to-metal transition.

APPENDIX B: HUBBARD MODEL FOR THE HYDROGEN MOLECULE

The model consists of two electrons that can be distributed over two sites denoted by $i = 1, 2$. The ground state $|GS\rangle$ of the system can be described as a linear combination of a state $|\varphi_0\rangle$ in which the two electrons are on different sites coupled to a singlet, and another singlet state $|\varphi_1\rangle$ in which both electrons are on the same site,

$$|GS\rangle = \alpha|\varphi_0\rangle + \beta|\varphi_1\rangle,$$

$$|\varphi_0\rangle = \frac{1}{\sqrt{2}}(c_{1\uparrow}^\dagger c_{2\downarrow}^\dagger + c_{2\uparrow}^\dagger c_{1\downarrow}^\dagger)|0\rangle,$$

$$|\varphi_1\rangle = \frac{1}{\sqrt{2}}(c_{1\uparrow}^\dagger c_{1\downarrow}^\dagger + c_{2\uparrow}^\dagger c_{2\downarrow}^\dagger)|0\rangle.$$

Here, $|0\rangle$ denotes the vacuum state out of which the operators $c_{i\sigma}^\dagger$ create an electron at site i with spin $\sigma = \uparrow, \downarrow$. The triplet states are not considered since they do not hybridize with each other to allow for the formation of a lower-energy state [49]. The coefficients α and β with $\alpha^2 + \beta^2 = 1$ are determined by diagonalizing the ground-state Hamiltonian,

$$\mathcal{H}_{GS} = \begin{pmatrix} 0 & 2t \\ 2t & U \end{pmatrix},$$

in which U denotes the on-site Coulomb repulsion between two electrons at the same site, and t is the hopping integral of the electron between the two sites.

1. Photoemission final states

The photoemission process, in which an electron is removed, is represented by the annihilation operators $c_{i\sigma}$. In a basis of states in which the remaining electron is localized at one of the two sites, $c_{i\sigma}^{\dagger}|0\rangle$, $i = 1, 2$, the final-state Hamiltonian and the corresponding eigenstates are given by

$$\mathcal{H}_{\mathrm{FS}} = \begin{pmatrix} 0 & t \\ t & 0 \end{pmatrix},$$

$$|\mathrm{FS}^{\pm}\rangle = \frac{1}{\sqrt{2}}(c_{1\sigma}^{\dagger} \pm c_{2\sigma}^{\dagger})|0\rangle.$$

These final states are the well-known bonding and anti-bonding states of the H_2^+ ion, which are separated in energy by $2t$. See Fig. 6.

2. Photoemission spectral weights

Depending on the spin of the removed photoelectron, the final states can take two spin orientations σ of equal energy. One can see immediately that the photoemission spectrum of this system consists of two lines associated with the two final states. The separation of the peaks in the spectrum is given by the final-state splitting $2t$. Their intensities depend only on the initial-state coefficients α and β. An exemplary spectrum is sketched in Fig. 6 on the right, with a lifetime broadening of the photoemission lines taken into account.

We calculate the spectrum as the intensity proportional to the square of the transition matrix elements for the photoemission process,

$$I^{\pm} \propto \|\langle FS^{\pm}|c_{i\sigma}|GS\rangle\|^2 = \frac{1}{4}|\alpha \pm \beta|^2$$
$$= \frac{1}{4}\left(1 \pm \sqrt{16t^2/(U^2 + 16t^2)}\right),$$

where we note that the sum of I^+ and I^- equals $1/2$. Since there are four photoemission operators $c_{i\sigma}$ for $i = 1, 2$ and $\sigma = \uparrow, \downarrow$, which naturally all yield the same spectral intensities, the total intensity equals 2, which is the number of electrons in the ground state of the system.

We thus find that the intensities only depend on the ratio between U and t, and we can immediately evaluate the relative intensities for two limiting cases. First, for $U = 0$, $\alpha = \beta = 1/\sqrt{2}$, and thus I^- vanishes. The spectrum is then given by a single line only. In other words, although there are two final states, we can only reach the lowest of them because of the fully constructive and fully destructive interference in the expression for the transition matrix elements. We are thus back to the one-electron approximation, essentially reproducing the results of band structure calculations. Second, for $U/t \to \infty$, $\alpha = 1$ and $\beta = 0$, and thus $I^+ = I^-$. The intensities for the two final states are then equal. In this limit, there is no double occupation in the ground state, and the two electrons reside on one site each.

The experimental spectrum for Ti_2O_3, as displayed in Fig. 1 in the main text, reveals that the energy separation between the satellite S and the main feature M is $2.43 - 0.68 = 1.75$ eV. In the hydrogen model, this corresponds to $2t$. In other words, $t \approx 0.88$ eV. The experimental spectrum in Fig. 1 also shows that the intensity ratio between S and M is about 0.15, so we can deduce a value of $U/t \approx 3$–4. We thus obtain $U \approx 2.5$–3.5 eV for Ti_2O_3.

APPENDIX C: CALCULATED VALENCE-BAND SPECTRA AS A FUNCTION OF THE INTER-TI HOPPING $dd\sigma$ USING THE Ti_2O_9 CLUSTER

Figure 7 shows the calculated valence-band photoemission spectra of Ti_2O_3 using the Ti_2O_9 cluster for several values of the inter-Ti hopping $dd\sigma$. The calculated energy
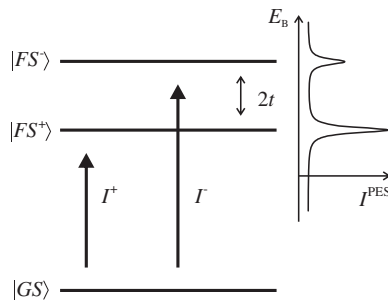

FIG. 6. Total-energy-level diagram for the photoemission process in a hydrogen molecule model. The two accessible final states $|\mathrm{FS}^+\rangle$ and $|\mathrm{FS}^-\rangle$ yield two lines in the spectrum of intensities I^+ and I^-, respectively, according to the initial-state coefficients α and β. The corresponding spectrum is indicated on the right.
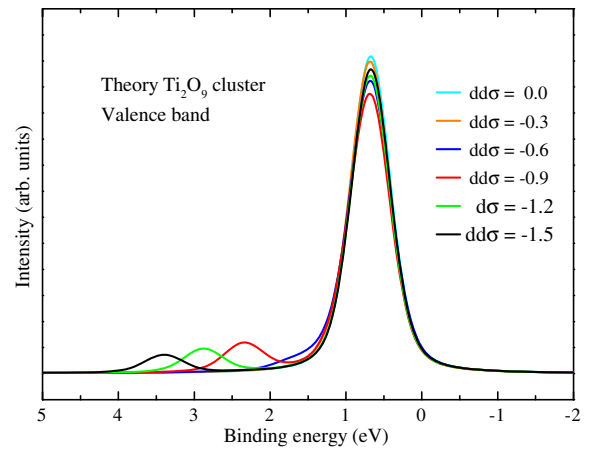

FIG. 7. Calculated valence-band photoemission spectra of Ti_2O_3 using the Ti_2O_9 cluster for several values of the inter-Ti hopping $dd\sigma$.

separation between the satellite S and the main peak M depends on the strength of the inter-Ti hopping $dd\sigma$. The stronger the $dd\sigma$, the larger the energy separation. We find that a $dd\sigma$ of -0.9 eV reproduces the experimental energy separation between S and M the best. This $dd\sigma$ value is very close to the value of $t \approx 0.88$ eV using the Hubbard hydrogen molecule model, as described in the section above. The S/M intensity ratio depends on the ratio of $dd\sigma$ and U, and it decreases slowly with increasing $dd\sigma$ for a fixed value of U.

———————

[1] J. B. Goodenough, *Direct Cation–Cation Interactions in Several Oxides*, Phys. Rev. **117**, 1442 (1960).

[2] L. L. Van Zandt, J. M. Honig, and J. B. Goodenough, *Resistivity and Magnetic Order in* Ti_2O_3, J. Appl. Phys. **39**, 594 (1968).

[3] H. J. Zeiger, *Unified Model of the Insulator-Metal Transition in* Ti_2O_3 *and the High-Temperature Transitions in* V_2O_3, Phys. Rev. B **11**, 5132 (1975).

[4] C. Castellani, C. R. Natoli, and J. Ranninger, *Magnetic Structure of* V_2O_3 *in the Insulating Phase*, Phys. Rev. B **18**, 4945 (1978).

[5] M. Abbate, F. M. F. de Groot, J. C. Fuggle, Y. J. Ma, C. T. Chen, F. Sette, A. Fujimori, Y. Ueda, and K. Kosuge, *Soft-X-Ray-Absorption Studies of the Electronic-Structure Changes through the* VO_2 *Phase Transition*, Phys. Rev. B **43**, 7263 (1991).

[6] M. Abbate, R. Potze, G. A. Sawatzky, C. Schlenker, H. J. Lin, L. H. Tjeng, C. T. Chen, D. Teehan, and T. S. Turner, *Changes in the Electronic Structure of* Ti_4O_7 *Across the Semiconductor-Semiconductor-Metal Transitions*, Phys. Rev. B **51**, 10150 (1995).

[7] T. M. Rice, in *Spectroscopy of Mott Insulators and Correlated Metals*, Springer Series in Solid-State Science Vol. 119, edited by A. Fujimore and Y. Tokura (Springer, Berlin, 1995).

[8] L. F. Mattheiss, *Electronic Structure of Rhombohedral* Ti_2O_3, J. Phys. Condens. Matter **8**, 5987 (1996).

[9] F. Mila, R. Shiina, F.-C. Zhang, A. Joshi, M. Ma, V. Anisimov, and T. M. Rice, *Orbitally Degenerate Spin-1 Model for Insulating* V_2O_3, Phys. Rev. Lett. **85**, 1714 (2000).

[10] J.-H. Park, L. H. Tjeng, A. Tanaka, J. W. Allen, C. T. Chen, P. Metcalf, J. M. Honig, F. M. F. de Groot, and G. A. Sawatzky, *Spin and Orbital Occupation and Phase Transition in* V_2O_3, Phys. Rev. B **61**, 11506 (2000).

[11] R. Shiina, F. Mila, F.-C. Zhang, and T. M. Rice, *Atomic Spin, Molecular Orbitals, and Anomalous Antiferromagnetism in Insulating* V_2O_3, Phys. Rev. B **63**, 144422 (2001).

[12] I. S. Elfimov, T. Saha-Dasgupta, and M. A. Korotin, *Role of c-axis Pairs in* V_2O_3 *from the Band-Structure Point of View*, Phys. Rev. B **68**, 113105 (2003).

[13] A. Tanaka, *On the Metal-Insulator Transitions in* VO_2 *and* Ti_2O_3 *from a Unified Viewpoint*, J. Phys. Soc. Jpn. **73**, 152 (2004).

[14] A. I. Poteryaev, A. I. Lichtenstein, and G. Kotliar, *Nonlocal Coulomb Interactions and Metal-Insulator Transition in* Ti_2O_3: *A Cluster* LDA $+$ DMFT *Approach*, Phys. Rev. Lett. **93**, 086401 (2004).

[15] V. Eyert, U. Schwingenschlögl, and U. Eckern, *Covalent Bonding and Hybridization Effects in the Corundum-type Transition-Metal Oxides* V_2O_3 *and* Ti_2O_3, Europhys. Lett. **70**, 782 (2005).

[16] S. Biermann, A. Poteryaev, A. I. Lichtenstein, and A. Georges, *Dynamical Singlets and Correlation-Assisted Peierls Transition in* VO_2, Phys. Rev. Lett. **94**, 026404 (2005).

[17] M. W. Haverkort, Z. Hu, A. Tanaka, W. Reichelt, S. V. Streltsov, M. A. Korotin, V. I. Anisimov, H. H. Hsieh, H.-J. Lin, C. T. Chen, D. I. Khomskii, and L. H. Tjeng, *Orbital-Assisted Metal-Insulator Transition in* VO_2, Phys. Rev. Lett. **95**, 196404 (2005).

[18] T. C. Koethe, Z. Hu, M. W. Haverkort, C. Schüßler-Langeheine, F. Venturini, N. B. Brookes, O. Tjernberg, W. Reichelt, H. H. Hsieh, H.-J. Lin, C. T. Chen, and L. H. Tjeng, *Transfer of Spectral Weight and Symmetry Across the Metal-Insulator Transition in* VO_2, Phys. Rev. Lett. **97**, 116402 (2006).

[19] H. Sato, A. Tanaka, M. Sawada, F. Iga, K. Tsuji, M. Tsubota, M. Takemura, K. Yaji, M. Nagira, A. Kimura, T. Takabatake, H. Namatame, and M. Taniguchi, *Ti 3d Orbital Change Across Metal-Insulator Transition in* Ti_2O_3: *Polarization-Dependent Soft X-ray Absorption Spectroscopy at Ti 2p Edge*, J. Phys. Soc. Jpn. **75**, 053702 (2006).

[20] M. Uchida, J. Fujioka, Y. Onose, and Y. Tokura, *Charge Dynamics in Thermally and Doping Induced Insulator-Metal Transitions of* $(Ti_{1-x}V_x)_2O_3$, Phys. Rev. Lett. **101**, 066406 (2008).

[21] O. Nájera, M. Civelli, V. Dobrosavljević, and M. J. Rozenberg, *Resolving the* VO_2 *Controversy: Mott Mechanism Dominates the Insulator-to-Metal Transition*, Phys. Rev. B **95**, 035113 (2017).

[22] F. J. Morin, *Oxides Which Show a Metal-to-Insulator Transition at the Neel Temperature*, Phys. Rev. Lett. **3**, 34 (1959).

[23] C. E. Rice and W. R. Robinson, *High-Temperature Crystal Chemistry of* Ti_2O_3: *Structural Changes Accompanying the Semiconductor-Metal Tranisiton*, Acta Crystallogr. Sect. B **33**, 1342 (1977).

[24] L. K. Keys and L. N. Mulay, *Magnetic Susceptibility Measurements of Rutile and the Magnéli Phases of the Ti-O System*, Phys. Rev. **154**, 453 (1967).

[25] R. M. Moon, T. Riste, W. C. Koehler, and S. C. Abrahams, *Absence of Antiferromagnetism in* Ti_2O_3, J. Appl. Phys. **40**, 1445 (1969).

[26] S. C. Abrahams, *Magnetic and Crystal Structure of Titanium Sesquioxide*, Phys. Rev. **130**, 2230 (1963).

[27] P. D. Dernier, *The Crystal Structure of* V_2O_3 *and* $(V_{0.962}Cr_{0.038})_2O_3$ *near the Metal-Insulator Transition*, J. Phys. Chem. Solids **31**, 2569 (1970).

[28] F. Iori, M. Gatti, and A. Rubio, *Role of Nonlocal Exchange in the Electronic Structure of Correlated Oxides*, Phys. Rev. B **85**, 115129 (2012).

[29] Y. Guo, S. J. Clark, and J. Robertson, *Electronic and Magnetic Properties of* Ti_2O_3, Cr_2O_3, *and* Fe_2O_3 *Calculated*

by the Screened Exchange Hybrid Density Functional, J. Phys. Condens. Matter **24**, 325504 (2012).

[30] V. Singh and J. J. Pulikkotil, *Electronic Phase Transition and Transport Properties of* Ti_2O_3, J. Alloys Compd. **658**, 430 (2016).

[31] J. M. Honig and T. B. Reed, *Electrical Properties of* Ti_2O_3 *Single Crystal*, Phys. Rev. **174**, 1020 (1968).

[32] J. M. Honig, *Nature of the Electrical Transition in* Ti_2O_3, Rev. Mod. Phys. **40**, 748 (1968).

[33] R. L. Kurtz and V. E. Henrich, *Surface Electronic Structure of Corundum Transition-Metal Oxides:* Ti_2O_3, Phys. Rev. B **25**, 3563 (1982).

[34] J. M. McKay, M. H. Mohamed, and V. E. Henrich, *Localized* $3p$ *Excitations in* $3d$ *Transition-Metal-Series Spectroscopy*, Phys. Rev. B **35**, 4304 (1987).

[35] K. E. Smith and V. E. Henrich, *Bulk Band Dispersion in* Ti_2O_3 *and* V_2O_3, Phys. Rev. B **38**, 5965 (1988).

[36] K. E. Smith and V. E. Henrich, *Resonant Photoemission in* Ti_2O_3 *and* V_2O_3: *Hybridization and Localization of Cation* $3d$ *Orbitals*, Phys. Rev. B **38**, 9571 (1988).

[37] T. Uozumi, K. Okada, and A. Kotani, *Electronic Structures of Ti and V Oxides: Calculation of Valence Photoemission and Bremsstrahlung Isochromat Spectra*, J. Phys. Soc. Jpn. **62**, 2595 (1993).

[38] T. Uozumi, K. Okada, A. Kotani, Y. Tezuka, and S. Shin, *Ti* $2p$ *and Resonant* $3d$ *Photoemission Spectra of* Ti_2O_3, J. Phys. Soc. Jpn. **65**, 1150 (1996).

[39] C. Lucovsky, J. W. Allen, and R. Allen, in *Physics of Semiconductors*, Conference Series No. 43, edited by B. L. H. Wilson (Institute of Physics, London, 1979), p. 465.

[40] E. Weschke, C. Laubschat, T. Simmons, M. Domke, O. Strebel, and G. Kaindl, *Surface and Bulk Electronic Structure of Ce Metal Studied by High-Resolution Resonant Photoemission*, Phys. Rev. B **44**, 8304 (1991).

[41] A. Sekiyama, T. Iwasaki, K. Matsuda, Y. Saitoh, Y. Onuki, and S. Suga, *Probing Bulk States of Correlated Electron Systems by High-Resolution Resonance Photoemission*, Nature (London) **403**, 396 (2000).

[42] A. Sekiyama, H. Fujiwara, S. Imada, S. Suga, H. Eisaki, S. I. Uchida, K. Takegahara, H. Harima, Y. Saitoh, I. A. Nekrasov, G. Keller, D. E. Kondakov, A. V. Kozhevnikov,

Th. Pruschke, K. Held, D. Vollhardt, and V. I. Anisimov, *Mutual Experimental and Theoretical Validation of Bulk Photoemission Spectra of* $Sr_{1-x}Ca_xVO_3$, Phys. Rev. Lett. **93**, 156402 (2004).

[43] A. Fujimori and F. Minami, *Valence-Band Photoemission and Optical Absorption in Nickel Compounds*, Phys. Rev. B **30**, 957 (1984).

[44] A. Tanaka and T. Jo, *Resonant* $3d$, $3p$ *and* $3s$ *Photoemission in Transition Metal Oxides Predicted at* $2p$ *Threshold*, J. Phys. Soc. Jpn. **63**, 2788 (1994).

[45] F. M. F. de Groot, *X-ray Absorption and Dichroism of Transition Metals and Their Compounds*, J. Electron Spectrosc. Relat. Phenom. **67**, 529 (1994).

[46] A. P. Hitchcock, G. E. McGuire, and J. J. Pireaux, *Theo Thole Memorial Issue*, J. Electron Spectrosc. Relat. Phenom. **86**, 1 (1997).

[47] A. E. Bocquet, T. Mizokawa, T. Saitoh, H. Namatame, and A. Fujimori, *Electronic Structure of 3d-Transition-Metal Compounds by Analysis of the* $2p$ *Core-Level Photoemission Spectra*, Phys. Rev. B **46**, 3771 (1992).

[48] TiO_6 cluster (eV): $U_{dd} = 4.0$, $U_{pd} = 5.5$, $\triangle = 6.5$, $10Dq_{ionic} = 0.85$, $\Delta_{trg} = -0.16$ for an e_g^π initial state and 0.16 for an a_{1g} initial state, hybridization $V_{eg}^\sigma = 3.5$, $V_{eg}^\pi = 1.2$, $V_{a_{1g}} = 0.9$. Ti_2O_9 cluster (eV): The hopping integral between two Ti atoms is simplified as a $V_{dd\sigma} = 0.9$, which is half of the energy difference between the $3d$ main peak (M) and the satellite (S) of the valence-band spectrum according to the H_2 Hubbard model. Otherwise, all parameters are the same as those used for the TiO_6 cluster. For calculating the $2p$ core-level photoemission spectrum, because of the presence of the core hole, $U_{pd} - U_{dd}$ is 5.5 eV for the Ti_2O_9 cluster.

[49] N. W. Ashcroft and N. D. Mermin, *Solid State Physics* (Holt-Saunders, Tokyo, 1981), Chap. 32, Problem 5.

[50] R. L. Kurtz and V. E. Henrich, *Comparison of Ti* $2p$ *Core-Level Peaks from* TiO_2, Ti_2O_3, *and Ti Metal, by XPS*, Surf. Sci. Spectra **5**, 179 (1998).

[51] I.-H. Hwang, B. Jiang, Z. Jin, C.-I. Park, and S.-W. Han, *Anomalous Structural Disorder and Distortion in Metal-to-Insulator-Transition* Ti_2O_3, J. Appl. Phys. **119**, 014905 (2016).